

## BEHAVIOUR OF OXYGEN BUBBLES DURING ALKALINE WATER ELECTROLYSIS

H. M. S. WEDERSHOVEN, R. M. DE JONGE, C. W. M. P. SILLEN and  
S. J. D. VAN STRALEN

Laboratory for Fluid Dynamics and Heat Transfer, Eindhoven University of Technology,  
Eindhoven, The Netherlands

(Received 11 May 1981)

**Abstract**—Growth rate, departure radius and population of oxygen bubbles at the transparent anode during alkaline water electrolysis have been investigated experimentally. The supersaturation of dissolved oxygen in the electrolyte adjacent to the anode surface has been derived from bubble growth rates. Ambient pressure (2–70 kPa) and molarity of the electrolyte (0.1–6.8 M KOH) are used as parameters.

### NOMENCLATURE

$B$ ,	bubble wetting parameter;
$\Delta C_0$ ,	initial supersaturation [ $\text{kmol m}^{-3}$ ] or [ $\text{kg m}^{-3}$ ];
$\Delta C_e$ ,	supersaturation of electrolyte at the electrode [ $\text{kmol m}^{-3}$ ] or [ $\text{kg m}^{-3}$ ];
$d$ ,	bubble density at electrode surface [ $\text{m}^{-2}$ ];
$D$ ,	diffusivity of oxygen in aqueous electrolyte [ $\text{m}^2 \text{s}^{-1}$ ];
$i$ ,	current density [ $\text{A m}^{-2}$ ];
$Ja$ ,	modified Jakob number, $\Delta C_0/\rho$ ;
$k$ ,	constant in Henry's law [ $\text{m}^2 \text{s}^{-2}$ ];
$R$ ,	gas bubble radius [ $\text{m}$ ];
$R_0$ ,	cavity mouth radius [ $\text{m}$ ];
$R_d$ ,	gas bubble departure radius [ $\text{m}$ ];
$p$ ,	ambient pressure [ $\text{Pa}$ ];
$t$ ,	time [ $\text{s}$ ].

### Greek symbols

$\beta$ ,	gas bubble growth parameter;
$\gamma$ ,	gas bubble mass growth parameter [ $\text{kg m}^{-3}$ ];
$\sigma$ ,	surface tension [ $\text{N m}^{-1}$ ];
$\rho$ ,	density of gas in bubble [ $\text{kg m}^{-3}$ ];
$\phi$ ,	contact angle.

### INTRODUCTION

DURING electrolysis of water, hydrogen (oxygen) gas bubbles are generated periodically on cavities at the cathode (anode) surface. The activation of these cavities is due to a supersaturation of gas in a liquid layer adjacent to the electrode.

The electrical resistance of the electrolyte between the electrodes is increased by the gas bubbles. For the practical purpose of limiting the corresponding increase in energetic losses, one must first study the bubble behaviour. This behaviour also determines the mass transport at the electrodes, the following quantities being important: nucleation properties of the electrode surface, bubble growth rates, departure time and radius, frequency and coalescence.

In the present study, the bubble population (depending on nucleation), growth rates and departure radius of oxygen bubbles are investigated. These bubbles are generated at the anode during water electrolysis in an alkaline solution in natural convection conditions. Current density, pressure and molarity of the electrolyte are used as parameters.

### EXPERIMENTAL PROCEDURE

#### Apparatus

The electrolysis vessel is shown in Fig. 1. The behaviour of electrolytically evolved oxygen bubbles has been studied by taking motion pictures through a microscope. As a consequence of the small field of view, high intensity illumination is required. Against the light photography has been used due to its advantage of giving optimal contrast of the bubble boundary with the surroundings (Chapter 7, ref. [1]). The gas bubbles are generated on transparent horizontal nickel electrodes. The electrodes are of a sandwich construction using a thin metallic layer, which adheres both to glass and to nickel. Figure 2 shows a roughness profile of the electrode surface, which is of importance for bubble nucleation and bubble population.

#### Procedure

If the electric current is switched on at a certain value, the electrolyte adjacent to the electrodes is supersaturated rapidly, causing bubble generation. The bubble measurements are made after approx. 30 min and are reproducible. Different results, especially an increased bubble density at the electrodes, are obtained if the current density is increased gradually to higher values and afterwards reduced to the original value [2]. This 'hysteresis' effect is similar to nucleate boiling (Chapter 11, ref. [1]).

### THEORETICAL BACKGROUND

#### Nucleation

A cavity with mouth radius,  $R_0$ , at the electrode surface acts as a nucleus for generating bubbles if the

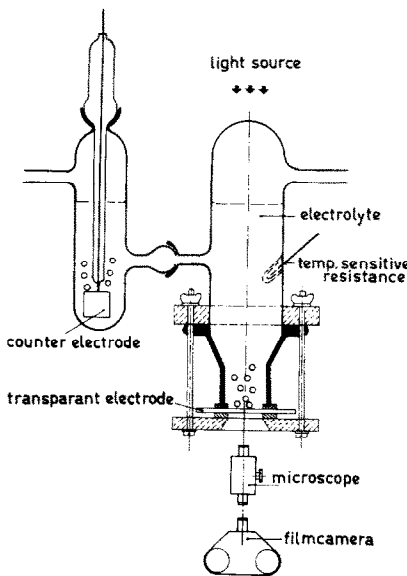


FIG. 1. Experimental set up for the study of the behaviour of oxygen bubbles, which are evolved at a horizontal, transparent, nickel electrode at natural convection.

following condition is satisfied (see Chapters 3-7, ref [1] for literature surveys):

$$R_0 \geq \frac{2\sigma}{\Delta p} = \frac{2\sigma}{k\Delta C_0}. \quad (1)$$

The shape, size, wettability and pretreatment and gas content of cavities determine their activation and their number and distribution on the electrode. As a consequence electrodes with a different surface roughness show different bubble populations at the same conditions, e.g. the electric current density: a rough surface has more favourable nucleation properties in comparison to a smooth surface. This is in accordance with equation (1).

With the present set up, the cavities are too small to be visualized. The roughness of the electrode surface is of the order of  $0.1 \mu\text{m}$ ; cavities of exactly this size are actually activated in  $0.1 \text{ M}$  aqueous alkaline solution at  $\Delta C_0 = 3 \times 10^{-2} \text{ kmol m}^{-3}$ . This value is calculated from equation (1). According to equation (1), relatively large cavities are activated at a relatively small supersaturation,  $\Delta C_0$ , i.e. at small electric current density  $i$ .

Also, the density of activated cavities at the electrode surface increases with increasing  $\Delta C_0$ . As a consequence, the ratio of the gas flux supplied directly to the bubbles adhering to the electrode to the total gas production rate increases from zero (in the region of

convection) to a saturation value, the maximum value in 'nucleate' electrolysis, at which film electrolysis occurs (Chapter 13, ref [1]).

#### Bubble growth

The growth of gas bubbles, generated during electrolysis is completely controlled by mass diffusion, as inertia effects can be neglected, due to the low value of the mass diffusion coefficient  $D$ , free gas bubbles in an infinite, initially uniformly supersaturated, non-viscous liquid grow according to [3]

$$R = 2\beta(Dt)^{1/2} \quad (2)$$

where

$$\beta = \beta(\Delta C_0) = \beta(Ja). \quad (3)$$

According to Buehl and Westwater [4], equation (3) holds also for a spherical bubble, which adheres to the electrode at the same conditions, with contact angle  $\phi=0$ ; the value of  $\beta$  for an adhering bubble has been decreased slightly in comparison to the value for a free bubble.

Both Zijl and van Stralen [5] and Verhaart, de Jonge and van Stralen [6], derived the following analytical expression for  $R(Ja)$ , with the modified Jakob number  $Ja = \Delta C_0/\rho$ , which is valid for free bubbles, in the transition region from low  $Ja \ll 1$  to high  $Ja \gg 1$ :

$$R(t) = (3/\pi)^{1/2} Ja [1 + (1 + \frac{2}{3}\pi/Ja)^{1/2}] (Dt)^{1/2}. \quad (4)$$

By combining equation (4) with the Buehl and Westwater model, de Jonge *et al.* [7] derived the following extension of equation (4), which is valid for adhering bubbles:

$$R(t) = (3/\pi)^{1/2} Ja [1 + (1 + \frac{2}{3}\pi \ln 2/Ja)^{1/2}] (Dt)^{1/2}. \quad (5)$$

Equation (5) has been used in the derivation of  $\Delta C_0$  from experimental  $R(t)$ -curves.

Equations (4) and (5) are of great value for electrolytically developed gas bubbles. In this case, small values of  $Ja$  occur, in comparison to vapour bubbles in nucleate boiling. For the investigated oxygen bubbles, the wetting is not complete, but still very good, as the average contact angle amounts to approximately  $\phi = 9 \times 10^{-2} \text{ rad}$ . According to van Stralen (Chapter 9, ref. [1]), the growth rate of a bubble with the shape of a spherical segment is reduced by a factor  $[B(3 - 2B)]^{-1}$ , which equals 0.996 for  $\phi = 9 \times 10^{-2} \text{ rad}$ ,  $B = \frac{1}{2}(1 - \cos \phi) = 0.998$ , i.e. the reduction in bubble growth rate is negligible here.

#### Liquid supersaturation

The supersaturation of the electrolyte at the electrode  $\Delta C_e$  is approximated by comparing the experimentally bubble growth rates with theory. Actually  $\Delta C_0 \leq \Delta C_e$ , as the supersaturation decreases with increasing distance to the electrode [8].

The supersaturation,  $\Delta C_0$ , vs current density  $i$ , is shown in Fig. 3. If  $i$  decreases, the bubbles generated on the active cavities, will carry away a too large quantity

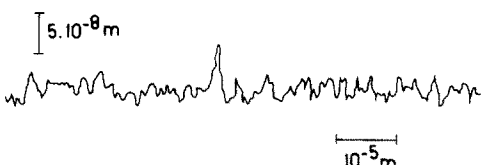


FIG. 2. Roughness profile of a transparent nickel electrode.

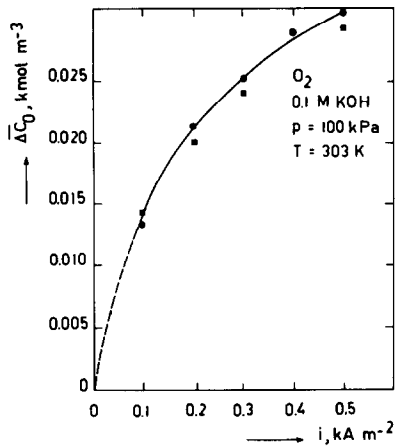


FIG. 3. Average supersaturation,  $\bar{\Delta}C_0$ , as a function of current density,  $i$ . The data have been obtained with the same transparent nickel anode.

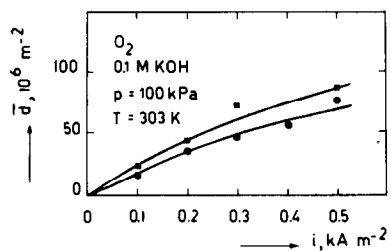


FIG. 4. Average bubble population,  $\bar{d}$ , as a function of current density,  $i$ . The data have been obtained with the same transparent nickel anode.

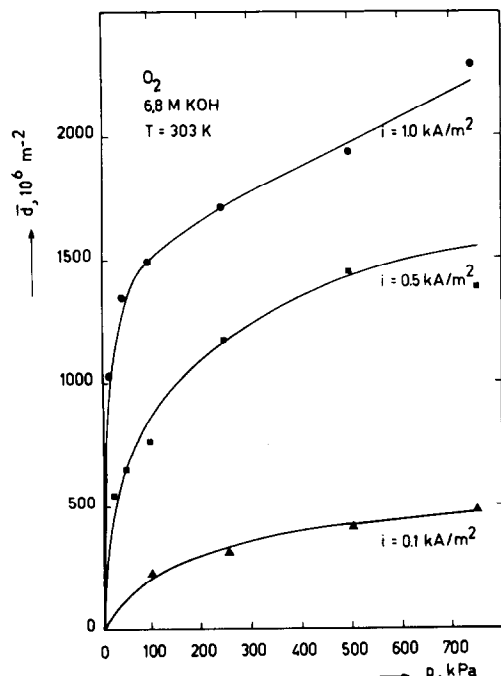


FIG. 6. Average bubble population,  $\bar{d}$ , as a function of pressure,  $p$ , with current density,  $i$ , as parameter. The data have been obtained with the same transparent nickel anode.

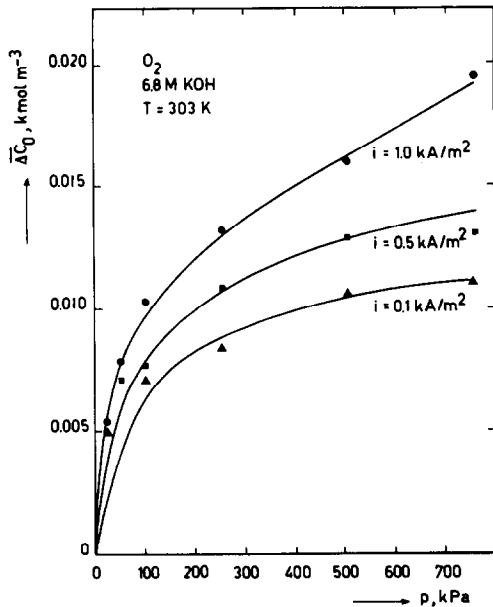


FIG. 5. Average supersaturation,  $\bar{\Delta}C_0$ , as a function of pressure,  $p$ , with current density,  $i$ , as parameter. The data have been obtained with the same transparent nickel anode.

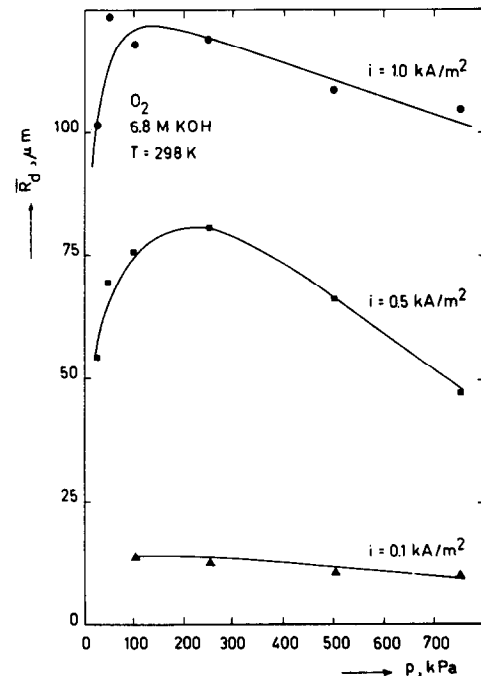


FIG. 7. Departure radius,  $\bar{R}_d$ , plotted vs pressure,  $p$ , with the current density,  $i$ , as parameter. The data have been obtained with the same transparent nickel anode.

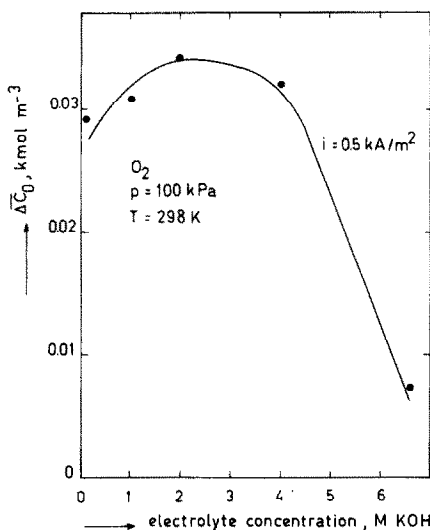


FIG. 8. Average supersaturation,  $\overline{\Delta C}_0$ , as a function of the electrolyte concentration. The experiments at 2 M KOH have been carried out with a different transparent nickel anode.

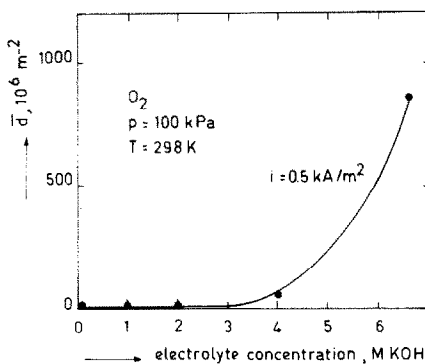


FIG. 9. Average bubble population,  $\bar{d}$ , as a function of the electrolyte concentration. The experiments at 2 M KOH have been carried out with a different transparent nickel anode.

of oxygen, which corresponds to the original value of  $i$ , and exceeds the value, corresponding to the actual (lower) value of  $i$ . As a consequence,  $\Delta C_0$  decreases and as a result the number of active cavities and thus the number of adhering bubbles, decreases (Fig. 4) until a new equilibrium at a lower value of  $\Delta C_0$  is reached.

The supersaturation,  $\Delta C_0$ , and the bubble population,  $d$ , have been determined several times at the same conditions. In this way, effects of properties of the various cavities or electrodes are averaged. The average values  $\Delta C_0$  and  $d$  are shown in the corresponding figures.

#### EXPERIMENTAL RESULTS

According to Figs. 5 and 6,  $\Delta C_0$  and  $d$  decrease at decreasing pressure. This effect can be explained qualitatively as follows: according to equations (2) and (3), the bubble mass growth rate is given by

$$\frac{4}{3} \pi \rho \frac{dR^3}{dt} = 16\pi\gamma D^{3/2} t^{1/2} \quad (6)$$

where

$$\gamma = \beta^3 \rho. \quad (7)$$

For very slowly growing bubbles,  $\beta \simeq (\Delta C_0/\rho)^{1/2}$  and so

$$\gamma \simeq (\Delta C_0)^{3/2}/\rho^{1/2}.$$

As a consequence, if  $p$  decreases,  $\gamma$  increases and the bubble consumes a larger quantity of gas from the surrounding liquid: this results in a decrease of  $\Delta C_0$ . In agreement with equation (1), the number of active cavities and thus  $d$  decreases also (Fig. 6).

At high pressures, a very large bubble population is observed, which exceeds  $10^9 \text{ m}^{-2}$ . In that situation, most of the bubbles leave the electrode surface by coalescing with neighbouring bubbles. This occurs already if the bubbles are still rather small. Consequently, at increase of  $p$ , the departure radius,  $R_d$ , decreases (Fig. 7). Only the largest bubbles are taken into account for Fig. 7.

The effect of the electrolyte concentration on  $\Delta C_0$  and  $d$  is shown in Figs. 8 and 9.  $\Delta C_0$  increases slightly in the trajectory of 0–3 M KOH. This could be caused by the fact that  $D$  decreases at higher concentrations [8]. The measuring with a high electrolyte concentration (6.8 M KOH) shows an increase of  $d$ . At this electrolyte concentration the value of  $\sigma/k$  is relatively low [10] and smaller cavities become active. As a result, because the amount of gas, produced at the electrode, remains the same at constant conditions,  $\Delta C_0$  decreases (Fig. 8).

#### REFERENCES

1. S. J. D. van Stralen and R. Cole, *Boiling Phenomena*, Hemisphere, Washington D.C., McGraw-Hill, New York (1979).
2. L. J. J. Janssen and S. J. D. van Stralen, Bubble behaviour on and mass transfer to an oxygen-evolving transparent nickel electrode in alkaline solution, *Electrochim. Acta* **26**, 1011–1022 (1981).
3. L. E. Scriven, On the dynamics of phase growth, *Chem. Engng Sci.* **10**, 1–13 (1959).
4. W. M. Buehl and J. W. Westwater, Bubble growth by dissolution: influence of contact angle, *A.I.Ch.E. J.* **12**, 571–576 (1966).
5. W. Zijl and S. J. D. van Stralen, Fundamental developments in bubble dynamics, *6th Int. Heat Transfer Conf.*, Toronto, Vol. 6, pp. 429–449 (1978).
6. H. F. A. Verhaar, R. M. de Jonge and S. J. D. van Stralen, Growth rate of a gas bubble during electrolysis in a supersaturated liquid, *Int. J. Heat Mass Transfer* **23**, 293–299 (1980).
7. R. M. de Jonge, E. Barendrecht, L. J. J. Janssen and S. J. D. van Stralen, Gas bubble behaviour and electrolyte Sources, *Tokyo* **1**, 195–207 (1980); *Int. J. Hydrogen Energy* **7**, to be published (1982).
8. H. Vogt, Physikalische Vorgänge an Gasentwickelnden Elektroden, *Chemie-Ingr-Tech.* **52**, 418–423 (1980).
9. R. E. Davis, G. L. Horvath and C. W. Tobias, The

solubility and diffusion coefficient of oxygen in potassium hydroxide solutions, *Electrochim. Acta* **12**, 287-297 (1967).

10. K. Feldkamp, Die Oberflächenspannung wässriger NaOH- und KOH-Lösungen, *Chemie-Ingr-Tech.* **41**, 1181-1183 (1969).

### COMPORTEMENT DES BULLES D'OXYGENE PENDANT L'ELECTROLYSE ALCALINE DE L'EAU

**Résumé**—La vitesse de croissance, le rayon au détachement et la population des bulles d'oxygène à une électrode transparente pendant l'électrolyse alcaline de l'eau sont étudiés expérimentalement. La sursaturation d'oxygène dissous dans l'électrolyte adjacent à la surface de l'anode est déduite de la vitesse de croissance des bulles. Les paramètres sont la pression ambiante (2 à 70 kPa) et la molarité de l'électrolyte (0,1 à 6,8 KOH molaire).

### DAS VERHALTEN VON SAUERSTOFFBLASEN BEI DER ELEKTROLYSE ALKALISCHEN WASSERS

**Zusammenfassung**—Wachstumsgeschwindigkeit, Ablöseradius und Anzahl von Sauerstoffblasen an der transparenten Anode bei der Elektrolyse alkalischen Wassers wurden experimentell untersucht. Die Übersättigung durch gelösten Sauerstoff im Elektrolyt an der Anoden-Oberfläche wurde aus den Blasenwachstums-Geschwindigkeiten bestimmt. Parameter bei den Untersuchungen waren Umgebungsdruck (2 bis 70 kPa) und Molarität des Elektrolyten (0,1 bis 6,8 M KOH).

### ПОВЕДЕНИЕ ПУЗЫРЬКОВ КИСЛОРОДА ПРИ ЭЛЕКТРОЛИЗЕ В ЩЕЛОЧНОЙ ВОДЕ

**Аннотация**—Экспериментально исследовались скорость роста, радиус отрыва и плотность пузырьков кислорода на прозрачном аноде при электролизе в щелочной воде. Перенасыщение электролита у поверхности анода растворенным кислородом определялось по скорости роста пузырьков. В качестве параметров использовались давление окружающей среды (от 2 до 70 КПа) и молярность электролита (от 0,1 до 6,8 молярных KOH).